



Electronic and magnetic properties of NiO surfaces from first-principles

Abdelnabi Ali Elamin*

Physics Department, Faculty of Science and Technology, Omdurman Islamic University, Omdurman, Sudan

*Corresponding author: A. A. Elamin (e-mail: aealamain2016@oiu.edu.sd).

Article history: Received 06 Dec. 2021, Received in revised form 18 Jan. 2022, Accepted 18 Jan. 2022

DOI: <https://doi.org/10.52981/fjes.v11i1.1732>

ABSTRACT Density functional theory (DFT) is used to study the electronic and magnetic properties of different surfaces of NiO. The electronic and magnetic properties of forming different surfaces of NiO such as (001), (110), (101), and (111) were studied using density functional theory calculations from the first principle used. Our result found that the band gap changed dramatically, and the spin projected density of state changed the dominations of the majority and minority of spin channels around the Fermi level, and the charge density of the bulk and NiO (111) surface is also discussed. However, the magnetic properties observed the increasing and decreasing spin magnetic moments and found significant magnetic moments for O atoms in the NiO (101) slab. These features lead to a surprisingly diverse set of different surface electronic structures. The study observed that DFT + U density functional theory might be a valuable method for high-throughput workflows that require reliable band gap predictions at a moderate computational cost.

Keywords: Density functional theory; Surface configuration; Magnetic moment; Bandgap

1. INTRODUCTION

A series of transition metal monoxides attract great interest to researchers due to their diverse electronic and magnetic properties such as MnO, FeO, CoO, and NiO with electronic configuration ranging from 3d⁵ to 3d⁸ respectively [1-5], which allows for a wide range of applications, for example, in electronics, spinning [6-9], energy storage [10-13], and heterogeneous catalysis [14-17]. The essential characteristic of NiO blocks is their anti ferromagnetic (AFM) character in the [111] direction. NiO has attracted great interest due to the high temperature of Neel at 523 K [18]. Small particles of AFM matter begin to behave differently from units of mass by exhibiting many new physical phenomena, such as super magnetism and weak ferromagnetism, as discussed by Neil [19].

NiO materials have also attracted great interest in solar energy conversion due to their

p-type character in the context of solar cells. Several combinations have been detected in p-type semiconductors of dye-sensitive solar cells (DSSCs) [20-22] and dye-sensitive photosynthesis cells (DSPECs) [23,24], in which holes are injected from the elongated molecule to the valence-band on the surface instead of of electron injection as in the conventional n-type system [25-27]. Surfaces bound every real solid, and specific processes happen on the surface. These include crystal growth, oxidation, adsorption, catalysis or etching. They cannot be described by the model of an infinite solid [28].

For a proper treatment of surface phenomena, knowledge of the surface properties is required. The surface itself can be thought of as a distinct physical object. Under normal conditions (room temperature, atmospheric pressure), the actual surface of a solid is far from the ideal system desirable for a proper physical study.

In this work, state of the art density functional theory (DFT) calculations was performed to investigate the electronic and magnetic properties for different surfaces of NiO (001), (101), (110) and (111).

In order to get a deep understanding of the behavior of electronic states and spin magnetic moments, which is an essential component of all spin devices such as magnetic tunnel junction (MTJ) and spin-transfer torque (STT) for predicting a new era of modern technology of spinronics. However, to improve the accuracy of the calculated electronic band gaps, the DFT+U (a corrective U term designed to restore the partial linearity of the energy sum associated with orbital occupations within a Hubbard manifold) was added to integrate electronic structure calculations.

Furthermore, playing of the spin degree of freedom became widely applicable to increasingly complex and realistic physical systems and devices, arriving well to the field of nanotechnology with applications ranging from metallic molecular junctions, field-effect transistors to carbon nanotubes, metallic or semiconductor nanostructures [29, 30]. Characterization of the building blocks properties will become of fundamental importance for such complex applications.

This paper is organized as follows. The first section presents a general introduction, including motivation and the primary goal. Section two shows the theoretical method employed here to calculate the electronic structure. In addition, computational details are also presented for the protocols used to generate slab models in first-principles calculations and structure optimization for the unit cell. In section three, the electronic and magnetic properties of the bulk NiO and different surfaces are also presented and discussed. Finally, the conclusion is drawn in section four.

II. COMPUTATIONAL DETAILS

To study the electronic structure and magnetic properties of the loose and clean (001), (101), (110), and (111) surfaces of a typical correlated insulator of NiO using the package QUANTUM ESPRESSO (QE) [31,32] with Hubbard correction.

In condensed matter physics, first-principles modelling of systems with local d states in our current study poses a major challenge. Stabilization of the DFT into the standard local density approximation (LDA) or generalized gradient approximation (GGA) is a major problem, which is best illustrated by the known failure of LDA/GGA for subsequent transition metal oxides [33].

In our present work, the convergence Hubbard U correction is 8.47 eV. The exchange-correlation energy and the core electrons are dealt with the ultra soft (USP), with linear response of PBEsol—the revised version of Perdew Burke-Ernzerh of exchange-correlation functional for solids [34]. For bulk nitrogen, the kinetic energy cutoff for the wave function 45 Ry was used, and the energy cutoff for the charge density was 480Ry, for the standard relative pseudo voltage. The Brillouin region was sampled using a k-dot $8 \times 8 \times 8$ Monkhorst-Pack grid [35].

However, the densest $24 \times 24 \times 24$ dot grid is used to calculate the expected density of states, with cold Marzari-Vanderbilt smearing displaying 0.00734. On the other hand, for the cleave NiO slabs, materials studio software was used, it is a complete simulation and modeling environment designed to allow researchers in materials science and chemistry to predict and understand the relationships of a substance's atomic and molecular structure to its properties and behavior. The equilibrium network constants for NiO surfaces were individually optimized using supercell models with a temporal vacuum area of at least 10 Å to ensure separation between adjacent plates based on the DFT.

The Brillouin region was sampled using a K-point $6 \times 6 \times 1$ Monkhorst-Pack grid [35]. However, the much denser mesh of $18 \times 18 \times 1$ k points is used to calculate the projected density of states. Electronic energy was converged to within 10⁻⁶Ry, and the atomic positions are relaxed until Hellman-Feynman forces on each atom are less than 0.001, 0.0009, 0.0006 and 0.0003 eV/Å for (001), (101), (110)and (111) in the slab model of NiO, respectively.

III. RESULTS AND DISCUSSION

Geometrical and structures of the NiO surfaces

Fig. 1 shows the most stable relaxed structures of different surfaces of NiO monolayer configuration. The converged lattice constants are

as follow: NiO(001), 2×2, ($a = b = 5.89\text{\AA}$), NiO(101), 2×2, ($a = 5.89\text{\AA}$ $b = 8.33\text{\AA}$), NiO(110), 2×2, ($a = 8.33\text{\AA}$ $b = 5.89\text{\AA}$) and NiO(111), 2×2, ($a = 5.89\text{\AA}$ $b = 5.89\text{\AA}$).

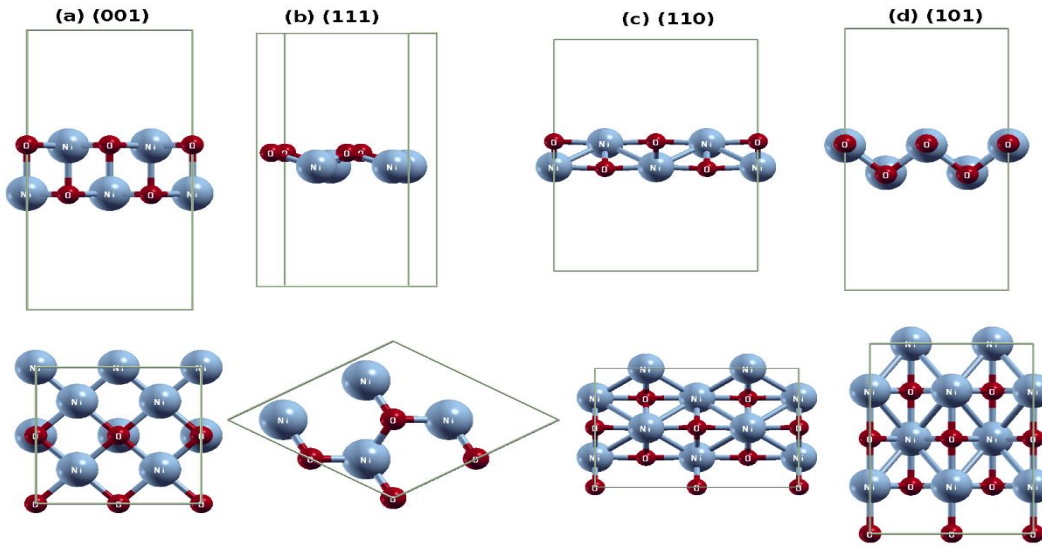


Fig. 1. The optimized local structure unit cell (top panel) (a) NiO(001), (b) NiO(111), (c) NiO(110) and (d) NiO(101).

The bottom panel shows the different side of view for the above slab models.

Our results find that the interlayer (vertical) distance is $d_{\text{Ni/O}} = 2.101\text{\AA}$ and (horizontal) distance is $d_{\text{Ni/O}} = 1.47\text{\AA}$ between the Ni and O atoms for NiO(001) [see Fig. 1(a)]. Furthermore, the vertical and horizontal distance for NiO(110) slab between Ni and O atoms are $d_{\text{Ni/O}} = 1.264\text{\AA}$, $d_{\text{Ni/O}} = 2.084\text{\AA}$, respectively. On the other hand, the distances between Ni and O atoms for NiO(111) and NiO(101) are $d_{\text{Ni/O}} = 0.607\text{\AA}$, $d_{\text{Ni/O}} = 1.273\text{\AA}$, respectively.

Magnetic properties ordering of the NiO

The possibility of developing magnetic devices by fabricating transition metal oxides has stimulated many experimental and theoretical groups to investigate the electronic and magnetic properties of these low-dimensional systems. Most of the experimental interest has focused on 3D ferromagnets such as Fe, Co, and Ni. It was noted that the current Stern-Gerlach techniques based on the deflection of the cluster beam due to its interaction with an inhomogeneous external magnetic field allows one to determine the average magnetization of each atom in the cluster. In order to understand the magnetic arrangement of our systems, the magnetic spin moments were

calculated in Table 1 for the NiO block and Table 2 for the NiO (001), (101) and (110) surface.

TABLE 1. THE SPIN MAGNETIC MOMENTS AT THE GROUND STATE ENERGY (E) FOR THE BULK NiO AND NiO(111) PLANE.

Atomic site	Magnetic moments (μ_B)	
	Bulk NiO	NiO(111)
Ni1	1.7829	1.5050
Ni2	1.7829	1.5051
Ni3	-1.7829	-1.5049
Ni4	-1.7829	-1.5049
O1	-0.0533	-0.0368
O2	-0.0533	-0.0371
O3	0.0533	0.0365
O4	0.0533	0.0365

One can see from Table 1 the magnetic moments for Ni atoms of the bulk behave as an anti-ferromagnetic character between 1.7829 to $-1.7829 \mu_B$ and decrease in the NiO(111) surface which between 1.50 to $-1.50 \mu_B$. And the O atoms became polarized with 0.0355 and $-0.0355 \mu_B$. On the other hand, in Table 2 all Ni atoms have same behavior of magnetic moments but with a positive and a negative sign of spin. Our results observed here a significant increase of the O

atoms magnetic moments especially for NiO(101) around $0.1098 \mu_B$.

TABLE 2. THE SPIN MAGNETIC MOMENTS AT THE GROUND STATE ENERGY (E) FOR THE NiO(001), NiO(101) AND NiO(110) SURFACES.

Atomic site	Magnetic moments (μ_B)		
	NiO(001)	NiO(101)	NiO(110)
Ni1	1.7199	1.6459	1.6404
Ni2	1.7200	1.6458	1.6404
Ni3	1.7200	1.6458	1.6404
Ni4	1.7200	1.6458	1.6404
Ni5	-1.7200	-1.6458	-1.6404
Ni6	-1.7200	-1.6457	-1.6405
Ni7	-1.7200	-1.6458	-1.6404
Ni8	-1.7200	-1.6457	-1.6404
O1	0.0383	0.1098	0.0134
O2	0.0384	0.1097	0.0135
O3	0.0383	0.1098	0.0135
O4	0.0384	0.1097	0.0135
O5	-0.0383	-0.1097	-0.0135
O6	-0.0383	-0.1097	-0.0134
O7	-0.0384	-0.1097	-0.0134
O8	-0.0383	-0.1097	-0.0134

Furthermore, the calculated magnetic moments for the NiO(001), NiO(110) and NiO(101) surfaces are shown in Table 2. Our results show that the

magnetic moments of Ni atoms fluctuate with parallel spin $1.7 \mu_B$ and opposite spin with $-1.7 \mu_B$. In addition to we find O atoms a bit big magnetic moments of $0.1 \mu_B$ in NiO (101) surface compared to other surface configurations.

Electronic properties of the different slab models of NiO

Electronic properties are a set of parameters and representations that fully describe the state and behavior of electrons in a material. For example, the electronic band structure [36], Here one is interested in the plate model of the anti-Neo magnetic order state and compares the electronic properties of the individual different surfaces in terms of predicted state density (PDOS) to show the shell (s, y, d, f) orbital of a given atom has the largest share in the total DOS and contributes to the electronic states in Our system, which describes the state of electrons in terms of their energy, E, and momentum, k. Electronic properties refer to physical quantities that are directly related to the response of charge carriers in an electric, magnetic, and electromagnetic field.

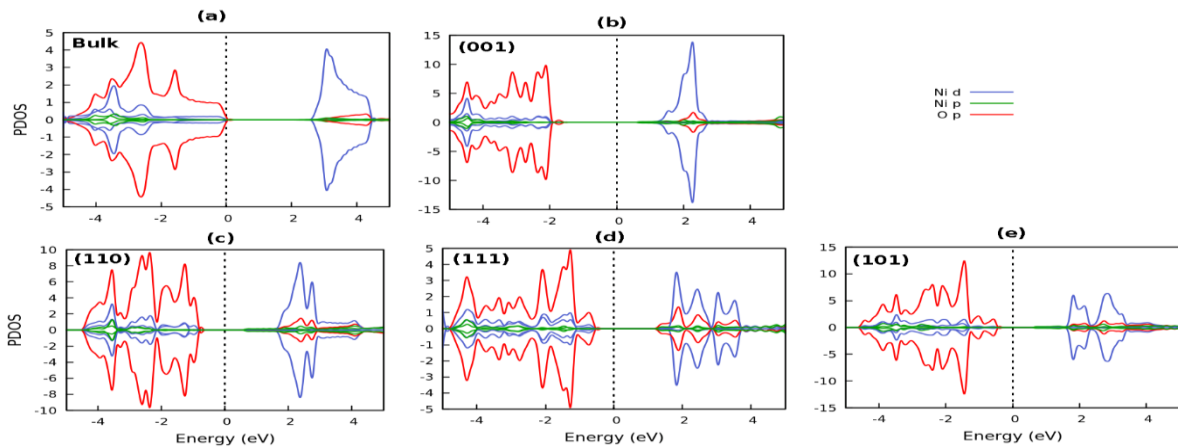


Fig. 2. The projected density of state (PDOS) for (a) Bulk NiO, (b) NiO(001), (c) NiO(110), (d) NiO(111) and (e) NiO (101).

The PDOS of h-BN (bottom panel), d and p-orbitals of Ni atoms, and p-orbital of O atoms at different slab models. Positive, and negative PDOS are for the spin up and spin down

channels, respectively. Vertical dashed lines indicate the Fermi level (EF).

Fig. 2 shows the majority (up spin) and minority (down spin) of the bulk NiO [see Fig. 2(a)] and different surfaces. It is clear that the bandgap changed dramatically for different planes

($E_g=1.678, 1.979, 2.342$ and 3.19 eV for (111), (101), (110) and (001)) of NiO and the denomination of the density of state by the d-orbital (blue line) of Ni and p-orbital (red line) of O atoms.

But our results observed significant DOS domination for NiO(111), which characterized by p-orbital around Fermi level with small band gap. In general, the necessity to apply the Hubbard U correction to specific states of a given item can be assessed by a PDOS examination of the material. In particular, the PDOS plots showed the specific states with the highest density of states (DOS) near the maximum valence band (VBM) and the lowest conduction band (CBM) in semiconductors and insulators.

The volumetric Charge density of the bulk NiO and NiO(111)

In order to complete the analysis of the electronic properties, especially for the bulk NiO and (111) surface, we have investigated the charge carries density as shown in Fig. 3. Which shows the corresponding carrier density near EF of the bulk

NiO and (111) surface, is the best choice to compare both structures' charge density distribution and chemical bonding properties due to the significant behaviour of orbitals near Fermi level as shown in Fig. 1.

Fig. 3(a) shows the charge density of bulk NiO. Our results observed that the higher charge density localized in the ion for Ni and O atoms according to the scale colour on the top left, in addition to the appearing of low density with yellow colour like pockets between ions, this result also confirms that bulk NiO is the insulator under DFT+U and there is no charge transfer between O and Ni atoms. On the other hand, Fig. 3(b) represents the charge density of the NiO(111) surface. Our results find that the O atoms are characterized by higher density than Ni atoms, different from the bulk charge density configurations. In general, the results of volumetric charge density agree well with the projected density of state in Fig. 2.

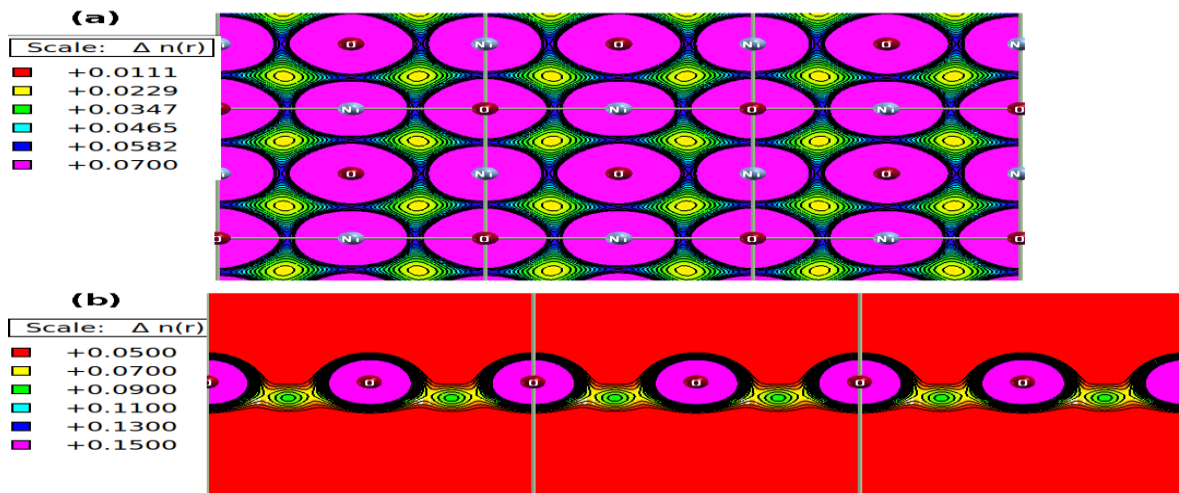


Fig. 3. Contour plots of the electronic 3D charge density distribution for (a) Bulk NiO and (b) NiO(111) plane. The surface value for the bulk NiO is $0.03e/\text{\AA}^3$ and $0.1e/\text{\AA}^3$ for NiO(111).

IV. CONCLUSION

In conclusion, we have presented an ab-initio study in the electronic and magnetic properties of the NiO(001), (110), (101) and (111) surfaces. Our result found that the band gap changed dramatically, and the spin projected density of state changed the dominations of the majority and minority of spin channels around the Fermi level, and the charge density of the bulk and NiO(111) surface is also discussed. However, the magnetic

properties observed the increasing and decreasing spin magnetic moments and found significant magnetic moments for O atoms in the NiO (101) slab.

REFERENCES

- [1] H. H. Kung, Transition Metal Oxides: Surface Chemistry and Catalysis (Elsevier, Amsterdam, 1989), Vol. 45.
- [2] V. E. Henrich and P. A. Cox, The Surface Science of Metal Oxides (Cambridge University Press, Cambridge, 1994).
- [3] C. Noguera, Physics and Chemistry of Oxide Surfaces (Cambridge University Press, Cambridge, 1996).

- [4] H.-J. Freund, H. Kuhlenbeck, and V. Staemmler, *Oxide surfaces*, Rep. Prog. Phys. 59, 283 (1996).
- [5] U. Kaiser, A. Schwarz, and R. Wiesendanger, Magnetic exchange force microscopy with atomic resolution, *Nature (London)* 446, 522 (2007).
- [6] Q. Liu, Q. Chen, Q. Zhang, Y. Xiao, X. Zhong, G. Dong, M.-P. Delplancke-Ogletree, H. Terryn, K. Baert, F. Reniers, and X. Diao, In situ electrochromic efficiency of a nickel oxide thin film: origin of electrochemical process and electrochromic degradation, *J. Mater. Chem. C* 6, 646 (2018).
- [7] W. Lin, K. Chen, S. Zhang, and C. L. Chien, Enhancement of Thermally Injected Spin Current through an Antiferromagnetic Insulator, *Phys. Rev. Lett.* 116, 186601 (2016).
- [8] E. Aytan, B. Debnath, F. Kargar, Y. Barlas, M. M. Lacerda, J. X. Li, R. K. Lake, J. Shi, and A. A. Balandin, Spin-phonon coupling in antiferromagnetic nickel oxide, *Appl. Phys. Lett.* 111, 252402 (2017).
- [9] M. Dabrowski, T. Nakano, D. M. Burn, A. Frisk, D. G. Newman, C. Klewe, Q. Li, M. Yang, P. Shafer, E. Arenholz, T. Hesjedal, G. van der Laan, Z. Q. Qiu, and R. J. Hicken, Coherent Transfer of Spin Angular Momentum by Evanescent Spin Waves within Antiferromagnetic NiO, *Phys. Rev. Lett.* 124, 217201 (2020).
- [10] P. L. S. G. Poizot, S. Laruelle, S. Grugeon, L. Dupont, and J. M. Tarascon, Nano-sized transition-metal oxides as negative-electrode materials for lithium-ion batteries, *Nature (London)* 407, 496 (2000).
- [11] M. V. Reddy, G. V. Subba Rao, and B. V. R. Chowdari, Metal oxides and oxysalts as anode materials for Li ion batteries, *Chem. Rev.* 113, 5364 (2013).
- [12] D. Su, M. Ford, and G. Wang, Mesoporous NiO crystals with dominantly exposed (110) reactive facets for ultrafast lithium storage, *Sci. Rep.* 2, 924 (2012).
- [13] D. U. Lee, J. Fu, M. G. Park, H. Liu, A. G. Kashkooli, and Z. Chen, Self-assembled NiO/Ni(OH)₂ nanoflakes as active material for high-power and high-energy hybrid rechargeable battery, *Nano Lett.* 16, 1794 (2016).
- [14] W. Zhao, M. Bajdich, S. Carey, and A. Vojvodic, Water dissociative adsorption on NiO(111): Energetics and structure of the hydroxylated surface, *ACS Catal.* 6, 7377 (2016).
- [15] A. Nelson, K. E. Fritz, S. Honrao, R. G. Hennig, R. D. Robinson, and J. Suntivich, Increased activity in hydrogen evolution electrocatalysis for partial anionic substitution in cobalt oxysulfide nanoparticles, *J. Mater. Chem. A* 4, 2842 (2016).
- [16] R. Poulain, A. Klein, and J. Proost, Electrocatalytic properties of (001)-, (110)-, and (111)-oriented NiO thin films toward the oxygen evolution reaction, *J. Phys. Chem. C* 122, 22252 (2018).
- [17] S. Gong, A. Wang, Y. Wang, H. Liu, N. Han, and Y. Chen, Heterostructured Ni/NiO nanocatalysts for ozone decomposition, *ACS Appl. Nano Mater.* 3, 597 (2020).
- [18] W. L. Roth, *Physical Review* 110, 1333 (1958).
- [19] L. Neel, in *Low Temperature Physics*, edited by C.
- [20] U. Bach, D. Lupo, P. Comte, J. E. Moser, F. Weissortel, J. Salbeck, H. Spreitzer, and M. Grätzel, *Nature* 395, 583 (1998).
- [21] A. Hagfeldt and M. Grätzel, *Accounts of Chemical Research* 33, 269 (2000).
- [22] M. Grätzel, *Nature* 414, 338 (2001).
- [23] L. Alibabaei et al., *Proceedings of the National Academy of Sciences* 110, 20008 (2013).
- [24] L. Alibabaei, H. Luo, R. L. House, P. G. Hoertz, R. Lopez, and T. J. Meyer, *Journal of Materials Chemistry A* 1, 4133 (2013).
- [25] J. He, H. Lindström, A. Hagfeldt, and S.-E. Lindquist, *The Journal of Physical Chemistry B* 103, 8940 (1999).
- [26] N. F. Mott, *Insulator Transitions* (Taylor & Francis, London, 1990).
- [27] M. Imada, A. Fujimori, and Y. Tokura, Metal-insulator transitions, *Rev. Mod. Phys.* 70, 1039 (1998).
- [28] F. Bechstedt, *Principles of Surface Physics*, Springer-Verlag (2003).
- [29] J. Hafner, C. Wolverton, and G. Ceder, *MRS Bulletin* 31, 659 (2006).
- [30] N. Marzari, *MRS Bulletin* 31, 681 (2006).
- [31] P. Hohenberg and W. Kohn, *Phys. Rev.* 136, B864 (1964).
- [32] P. Giannozzi, S. Baroni, N. Bonini, M. Calandra, R. Car, C. Cavazzoni, D. Ceresoli, G. L. Chiarotti, M. Cococcioni, I. Dabo, A. Dal Corso, S. de Gironcoli, S. Fabris, G. Fratesi, R. Gebauer, U. Gerstmann, C. Gougoussis, A. Kokalj, M. Lazzeri, L. Martin-Samos, N. Marzari, F. Mauri, R. Mazzarello, S. Paolini, A. Pasquarello, L. Paulatto, C. Sbraccia, S. Scandolo, G. Sclauzero, A. P. Seitsonen, A. Smogunov, P. Umari, and R. M. Wentzcovitch, *J. Phys. Condens. Matter* 21, 395502 (2009).
- [33] K. Terakura, T. Oguchi, A. R. Williams, and J. Kübler, *Physical Review B* 30, 4734 (1984).
- [34] J. P. Perdew, K. Burke, and M. Ernzerhof, *Phys. Rev. Lett.* 77, 3865 (1996).
- [35] H. J. Monkhorst and J. D. Pack, *Phys. Rev. B* 13, 5188 (1976).
- [36] N. W. Ashcroft, and N. D. Mermin: *Solid State Physics*, Holt-Saunders International Editions, ISBN 0030839939 London (1976).